

Geophysical Research Letters®



RESEARCH LETTER

10.1029/2023GL103742

Key Points:

- Trends in heavy summer precipitation over the southern slope of the Tibetan Plateau are positive in 1979–1996 and negative in 1996–2022
- Stratospheric ozone depletion led to lower stratospheric cooling and a reduction of upper-tropospheric static stability
- Stratospheric ozone depletion enhanced the deep convection and precipitation over the southern slope of the Tibetan Plateau

Supporting Information:

Supporting Information may be found in the online version of this article.

Correspondence to:

C. Zhao,
cfzhao@pku.edu.cn

Citation:

Xia, Y., Hu, Y., Huang, Y., Bian, J., Zhao, C., Lin, J., et al. (2023). Stratospheric ozone loss enhances summer precipitation over the southern slope of the Tibetan Plateau. *Geophysical Research Letters*, 50, e2023GL103742. <https://doi.org/10.1029/2023GL103742>

Received 17 MAR 2023

Accepted 1 AUG 2023

Author Contributions:

Conceptualization: Yan Xia

Formal analysis: Yan Xia








Investigation: Yan Xia

Methodology: Yan Xia

Writing – original draft: Yan Xia

Writing – review & editing: Yan Xia

Stratospheric Ozone Loss Enhances Summer Precipitation Over the Southern Slope of the Tibetan Plateau

Yan Xia^{1,2} , Yongyun Hu³ , Yi Huang⁴ , Jianchun Bian^{2,5,6} , Chuanfeng Zhao³ , Jintai Lin³ , Fei Xie¹ , and Chunjiang Zhou⁷

¹School of Systems Science, Beijing Normal University, Beijing, China, ²Key Laboratory of Middle Atmosphere and Global Environment Observation, Institute of Atmospheric Physics, Chinese Academy of Sciences, Beijing, China, ³Laboratory for Climate and Ocean-Atmosphere Studies, Department of Atmospheric and Oceanic Sciences, School of Physics, Peking University, Beijing, China, ⁴Department of Atmospheric and Oceanic Sciences, McGill University, Montreal, Quebec, Canada, ⁵College of Earth and Planetary Sciences, University of Chinese Academy of Sciences, Beijing, China, ⁶College of Atmospheric Sciences, Lanzhou University, Lanzhou, China, ⁷School of Ecology and Environment, Inner Mongolia University, Hohhot, China

Abstract Heavy summer precipitation over the southern slope of the Tibetan Plateau has dramatic influences on water resources and hydrological disasters in South Asia. It experienced increasing trends over 1979–1996 and decreasing trends over 1996–2022, which are not yet well understood. Here we show observational and numerical evidence that stratospheric ozone has significant impacts on long-term trends of summer precipitation in this strong convection area. It is found that stratospheric ozone depletion, by modulating the lower stratospheric temperature and upper-tropospheric static stability, enhances deep convection and precipitation over the southern slope of the Tibetan Plateau. The results suggest that the ozone recovery in the future may reduce the summer precipitation over the southern slope of the Tibetan Plateau in the first half of the 21st century, which would be imperative for future water resource management in South Asia.

Plain Language Summary South Asia, with a population of more than 1.8 billion, is among the most vulnerable regions in the world in response to climate change and a global hotspot for water security. Heavy summer precipitation over the southern slope of the Tibetan Plateau, which directly affects North India and Nepal with a population of more than 200 million and has dramatic influences on water resources and hydrological disasters in South Asia, experienced increasing trends over 1979–1996 and decreasing trends over 1996–2022 (Figure 1). We find that the long-term variations of the summer precipitation are likely related to the stratospheric ozone depletion and recovery over the Tibetan Plateau in recent decades. The convective precipitation over the southern slope of the Tibetan Plateau is modulated by the upper tropospheric static stability which is affected by the lower-stratospheric temperature. We find that stratospheric ozone depletion, which radiatively cools the lower stratosphere, enhances the deep convection and precipitation. This work helps to understand the stratospheric contributions to the changes in the summer precipitation over the southern slope of the Tibetan Plateau and future water resource management in South Asia.

1. Introduction

South Asia, with a population of more than 1.8 billion, is among the most vulnerable regions in the world in response to climate change (Bandara & Cai, 2014) and a global hotspot for food insecurity (Lal, 2013). The large populations across South Asia are dependent on summer precipitation for agriculture, hydroelectric generation, industrial development, and basic human needs (Turner & Annamalai, 2012). Both observations and model simulations show that heavy summer precipitation occurs along the southern slope of the Tibetan Plateau (TP, as shown in Figure S1 in Supporting Information S1), which has dramatic impacts on the landslide risk, water resources, and water security (water for drinking, ecosystems, hazard resilience) in South Asia and is found to influence the monsoon circulation through the teleconnection associated with the local latent heat flux (Bao & Li, 2020; Houze Jr. et al., 2007; Sharma et al., 2020). Previous studies have found that this heavy precipitation is associated with the deep convective systems over the TP, which is a part of the Asian Summer Monsoon (Gao et al., 2019; Grossman & Garcia, 1990; Qie et al., 2014; Romatschke & Houze, 2011; Romatschke et al., 2010; Wang et al., 2018). Summer precipitation on the TP, which is found to be influenced by Asian Summer Monsoons and the mid-latitude westerlies (Feng & Zhou, 2012; Schiemann et al., 2009; Webster et al., 1998), tropical

© 2023 The Authors.

This is an open access article under the terms of the [Creative Commons Attribution-NonCommercial License](https://creativecommons.org/licenses/by-nc/4.0/), which permits use, distribution and reproduction in any medium, provided the original work is properly cited and is not used for commercial purposes.

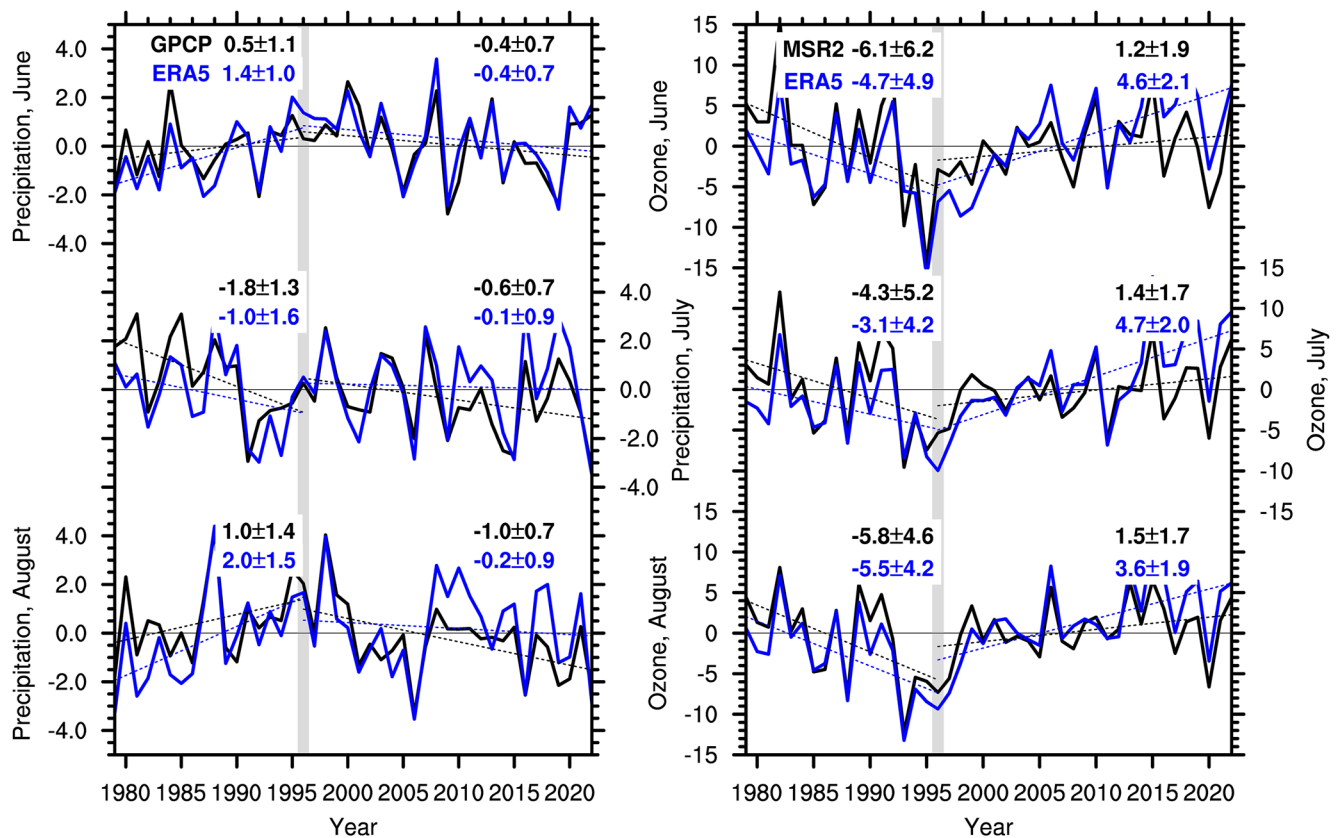


Figure 1. Time series of the precipitation (left panels) and total column ozone (right panels) anomalies averaged over the southern slope of the TP in June, July, and August over 1979–2022. In the left column, the black and blue lines indicate the precipitation in the GPCP and ERA5, respectively. In the right column, the black and blue lines indicate the total column ozone in the MSR-2 and ERA5, respectively. The units are mm/day in the left panels and DU in the right panels. Two piecewise linear trend lines (dashed lines) are drawn for the periods 1979–1996 and 1996–2022 in the GPCP (black) and ERA5 (blue) in the left panels and in the MSR-2 (black) and ERA5 (blue) in the right panels (the values for their slopes are provided in each panel with two σ uncertainties, units: mm/day/decade in the left column and DU/decade in the right column). DU, Dobson Unit. The gray-filled bar indicates year 1996.

oceanic processes (Cherchi & Navarra, 2013; Fasullo & Webster, 2002), the North Atlantic Oscillation (Liu & Yin, 2001; Liu et al., 2015), land surface status (Seneviratne et al., 2010), and aerosols (Choudhury et al., 2020; Zhao et al., 2019), generally shows an increasing trend during recent several decades over the northern TP (Wang et al., 2018). We find that the heavy precipitation over the southern slope of the TP, which mostly comes from convective precipitation (Wang et al., 2018), has a positive trend during 1979–1996 and a negative trend during 1996–2022 (Figure 1). The external forcings accounting for this long-term precipitation change are not yet well understood.

Stratospheric ozone over the TP experienced negative trends during the last several decades in the 20th century as a result of anthropogenic emission of ozone-depleting substances and positive trends in the recent two decades due to the successful implementation of the Montreal Protocol (Li et al., 2020; Zou et al., 2020). Here, we find that trends in the heavy precipitation over the southern slope of the TP during both the ozone depletion and recovery periods have opposite signs (Figure 1), yet this stratospheric ozone change-induced convective precipitation response has little been studied.

Recent studies have demonstrated that stratospheric anomalies can impact convective precipitation through temperature-mediated stability changes in the upper troposphere (Hu et al., 2021; Huangfu et al., 2021; Kim et al., 2020; Lim et al., 2019; Martin et al., 2021; Nie & Sobel, 2015; Yoshida & Mizuta, 2021; Zhang & Zhang, 2018). The influence of the stratospheric quasi-biennial oscillation (QBO) on the Madden–Julian oscillation convection has drawn extensive studies (Martin et al., 2021; Son et al., 2017; Yoo & Son, 2016), which have the potential to improve predictability. Sudden stratospheric warmings (SSWs), which drive polar warming and tropical cooling, are found to be able to affect tropical convection (Yoshida & Mizuta, 2021). It has been

suggested that both QBO and SSWs, which modulate the lower-stratospheric temperature and upper-tropospheric static stability, have significant impacts on deep convection, yet the influence of stratospheric anomalies on deep convection over the south slope of the Tibetan Plateau has not been studied.

A series of recent studies (Hu et al., 2019; Xia, Hu, Huang, Bian, & Zhao, 2021; Xia, Hu, Huang, Zhao, et al., 2021; Xia et al., 2016, 2018, 2020) have shown that the changes in lower-stratospheric ozone significantly influence the static stability in the upper troposphere and consequent variations of high clouds, which further impact surface temperature and ultraviolet radiation especially in the polar regions. Thus, the stratospheric ozone depletion and recovery may influence deep convection and precipitation over the southern slope of the TP by modifying the upper tropospheric stability, which warrants detailed investigation. In this study, we analyze how precipitation over the southern slope of the TP is related to stratospheric ozone change by both statistical analysis and model simulations. In Section 2, we address the data and numerical experiments analyzed in this study. In Section 3, we first show observational changes in the precipitation and stratospheric ozone over the southern slope of the TP. Next, we analyze how the precipitation change is related to stratospheric ozone loss using both the ERA5 reanalysis and sensitivity experiments.

2. Data and Experiments

2.1. ERA5 Reanalysis

The monthly mean ozone, temperature, fraction of cloud cover, winds, precipitation, and downward UV radiation at the surface are obtained from the ERA5 reanalysis over 1979–2022. ERA5, which is the fifth generation ECMWF reanalysis for the global climate and weather, combines model data with observations from across the world into a globally complete and consistent data set (Hersbach et al., 2020). A significantly more advanced 4D-var assimilation scheme is used to produce the analysis at a 1-hourly time step. The datasets have a horizontal resolution of $0.25^\circ \times 0.25^\circ$ with 37 pressure levels from 1,000 hPa to 1 hPa. Yao et al. (2020) evaluated the performances of ERA5 on representing cloud cover using MODIS product and found that ERA5 can give monthly mean cloud cover quite accurately.

2.2. The CESM2-CAM6 Model

To examine the impact of lower-stratospheric ozone on the precipitation over the TP, we perform sensitivity experiments using the atmospheric component of CESM2. CESM2 is the most current-generation Earth system model developed by the National Center for Atmospheric Research (NCAR) (Danabasoglu et al., 2020). CAM6 is the atmospheric component of CESM2 with a fully interactive aerosol scheme. In this study, CAM6 is performed at a horizontal resolution of $1.9^\circ \times 2.5^\circ$ with 32 vertical levels. The Zhang and McFarlane (1995) deep convective parameterization is used in CAM6 and it has been substantially retuned compared to its predecessor, such as reducing the number of negative buoyancy regions allowed.

We conduct two experiments of CAM6 simulations, including control and ozone-loss experiments. The two experiments differ only in prescribed ozone concentration. The control experiment is performed with ozone prescribed to year-2000 values. The ozone-loss experiment has settings similar to the control experiment, except that the ozone has negative anomalies between 150 and 50 hPa over 20° – 40° N. To obtain similar lower-stratospheric cooling to the long-term trends during 1979–1996, the ozone differences between the ozone-loss and control experiments are prescribed as shown in Figures 4a–4c. We can isolate the effect of the lower-stratospheric ozone over the TP by comparing the ozone-loss and control experiments. All the experiments are integrated for 50 years after equilibrium and the last 40 years are used for the analysis.

2.3. Observations

To confirm the impact of lower-stratospheric ozone on high clouds, surface UV radiation, and precipitation, the satellite observations of cloud fraction, surface UV radiation, and precipitation, and the monthly mean total column ozone from the Multi Sensor Re-analysis version 2 (MSR-2) are also used here. The MSR-2, constructed using all available satellite observations and surface observations, has a horizontal resolution of $0.5^\circ \times 0.5^\circ$ (Van Der A et al., 2015a, 2015b). High clouds (cloud fraction above 400 hPa) are obtained from Clouds and the Earth's Radiant Energy System (CERES) Synoptic (SYN1deg) product. CERES SYN1deg provides monthly

mean high clouds on a $1^\circ \times 1^\circ$ grid over March 2000–2019 (Doelling et al., 2013, 2016; Rutan et al., 2015). We use the surface UV irradiance from Ozone Monitoring Instrument (OMI) daily Level 3 (L3) gridded data product. OMI is a satellite instrument on board the NASA EOS-Aura satellite, in orbit since 2004 (Levelt et al., 2006). The surface UV irradiance and Erythral Dose from the Level-3 OMI/Aura has a horizontal resolution of $1^\circ \times 1^\circ$. The precipitation datasets are obtained from the Global Precipitation Climatology Project (GPCP) over 1979–2022 and the Tropical Rainfall Measuring Mission (TRMM) products 3B42 over 1998–2019. The GPCP Monthly product, with a spatial resolution of $2.5^\circ \times 2.5^\circ$, provides a consistent analysis of global precipitation from an integration of various satellite data sets over land and ocean and a gauge analysis over land (Adler et al., 2003; Huffman et al., 2009). The TRMM 3B42 product, with a spatial resolution of $0.25^\circ \times 0.25^\circ$, merges precipitation radar and microwave rainfall estimates with infrared-based precipitation estimates from multiple satellites, as well as measurements from rain gauges (Huffman et al., 2007).

3. Results

Figure 1 shows the time series of the precipitation and total column ozone anomalies averaged over the southern slope of the TP in June, July, and August (JJA) over 1979–2022. The anomalies are defined as relative to the 1979–2022 reference period. It is found that the variations of precipitation in the ERA5 are highly correlated with that in the GPCP, which can reach about 0.89. We find that the long-term variations of precipitation in the ERA5 are similar to that in the GPCP. In June and August, the precipitation experienced increasing trends over 1979–1996, which are 0.5 ± 1.1 (1.4 ± 1.0) and 1.0 ± 1.4 (2.0 ± 1.5) mm/day/decade in the GPCP (ERA5), respectively. Over 1996–2022, the precipitation trends are -0.4 ± 0.7 (-0.4 ± 0.7) and -1.0 ± 0.7 (-0.2 ± 0.9) mm/day/decade in June and August, respectively. This reversal of the long-term trend in precipitation since 1996 is consistent with the variations of stratospheric ozone. The ozone in the southern slope of the TP has negative trends during 1979–1996 and positive trends during 1996–2022, which implies a possible linkage between ozone and precipitation. The correlation coefficients between precipitation and ozone are significantly negative over 1979–2022 with 44 samples, which can reach about -0.40 , -0.41 , and -0.48 in June, July, and August, respectively. These results raise an important question: how the ozone changes influence the precipitation over the southern slope of the TP. In the following, we are motivated to answer this question based on statistical analysis and model simulations.

The significant correlation coefficients between the total column ozone and high clouds suggest that the stratospheric ozone and tropospheric convection are robustly coupled over the southern slope of the TP where the high clouds are significantly negatively correlated with the total column ozone due to the ozone-related temperature stratification effects (Figures S2a–S2c in Supporting Information S1). The climatological spatial pattern shows that the southern slope of the TP is covered by plenty of high clouds with a maximum value of about 89% (Figure S3 in Supporting Information S1). Stratospheric ozone loss generally allows more ultraviolet radiation (UV) radiation to reach the surface. The cloud scattering effects, which have an opposite impact on surface UV, lead to the significantly positive correlation coefficients between the total column ozone and surface UV radiation over the southern slope of the TP (Figures S2d–S2f in Supporting Information S1). This result is consistent with the previous study (Xia, Hu, Huang, Bian, & Zhao, 2021) and confirms the stratospheric-tropospheric coupling over the southern slope of the TP.

Figure 2 shows the long-term trends of ozone, temperature, static stability, and clouds with winds averaged over 75° – 95° E in JJA during 1979–1996. During this time period, ozone experienced significant depletion over the TP (Figures 3a–3c), especially between 70 and 10 hPa (Figures 2a–2c). The ozone depletion, which can reach about -0.7 ppm/decade at around 20 hPa, leads to significant cooling in the lower stratosphere with a maximum cooling rate of about -1.8 K/decade at about 70 hPa (Figures 2d–2f). The temperature trends in the troposphere are almost insignificant in summer. The lower-stratospheric cooling reduces the static stability in the upper troposphere (Figures 2g–2i) and results in the increase of tropospheric clouds and enhancement of deep convection over 24° – 28° N, 16° – 24° N, and 24° – 30° N in June, July, and August, respectively (Figures 2j–2l). The enhancement of the convection is located over the southern slope of the TP where strong climatological ascending motion occurs (Figure S4 in Supporting Information S1). The cloud increases throughout the whole tropospheric column (from surface to 100 hPa) with maximum values of about 4.2%, 8.8%, and 7.7%/decade in June, July, and August, respectively, at about 150 hPa.

Figures 3d–3l show the long-term trends of high clouds, surface downward UV radiation, and precipitation in June, July, and August during 1979–1996. The cloud increase corresponds to the reduction of the surface UV radiation in spite of the stratospheric ozone depletion (Figures 3d–3i). The enhancement of deep convection is

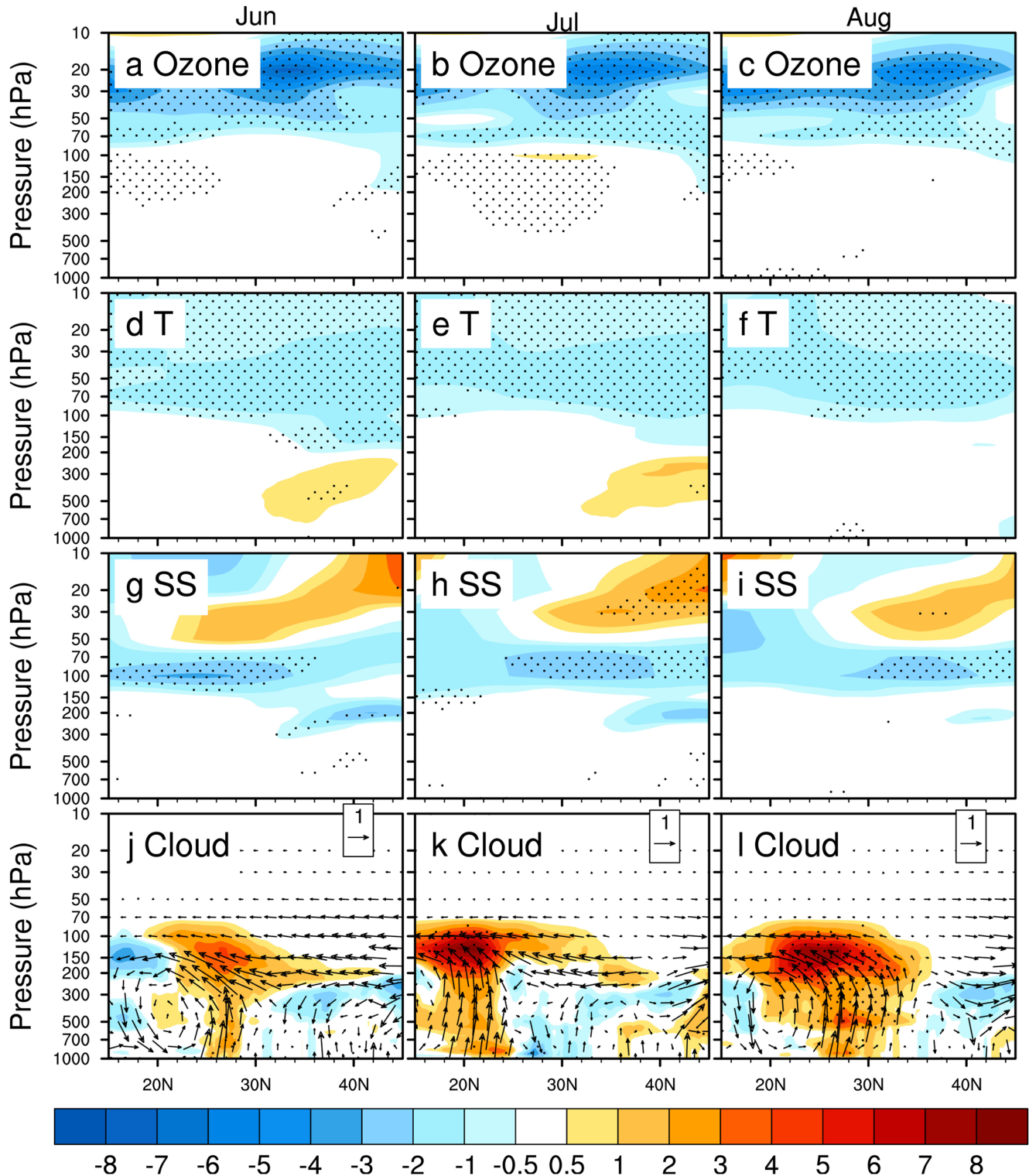


Figure 2. Vertical cross-section of long-term trends of (a–c) ozone, (d–f) temperature (T), (g–i) static stability (SS), and (j–l) cloud cover (color contours) with winds (vectors) averaged over 75°–95°E during 1979–1996 in June (Jun), July (Jul), and August (Aug) based on ERA5 reanalysis. The unit of panels (a–c) is 10^{-1} ppm/decade, (d–f) is K/decade, (g–i) is 10^{-2} K/hPa/decade, and then (j–l) is %/decade, and they share the same colormap. In (j–l), the units are m/s/decade and 10 hPa/day/decade for the meridional and vertical winds, respectively. Regions with dots are the places where regressions have statistical significance levels higher than the 95% confidence level based on the Student's *t*-test.

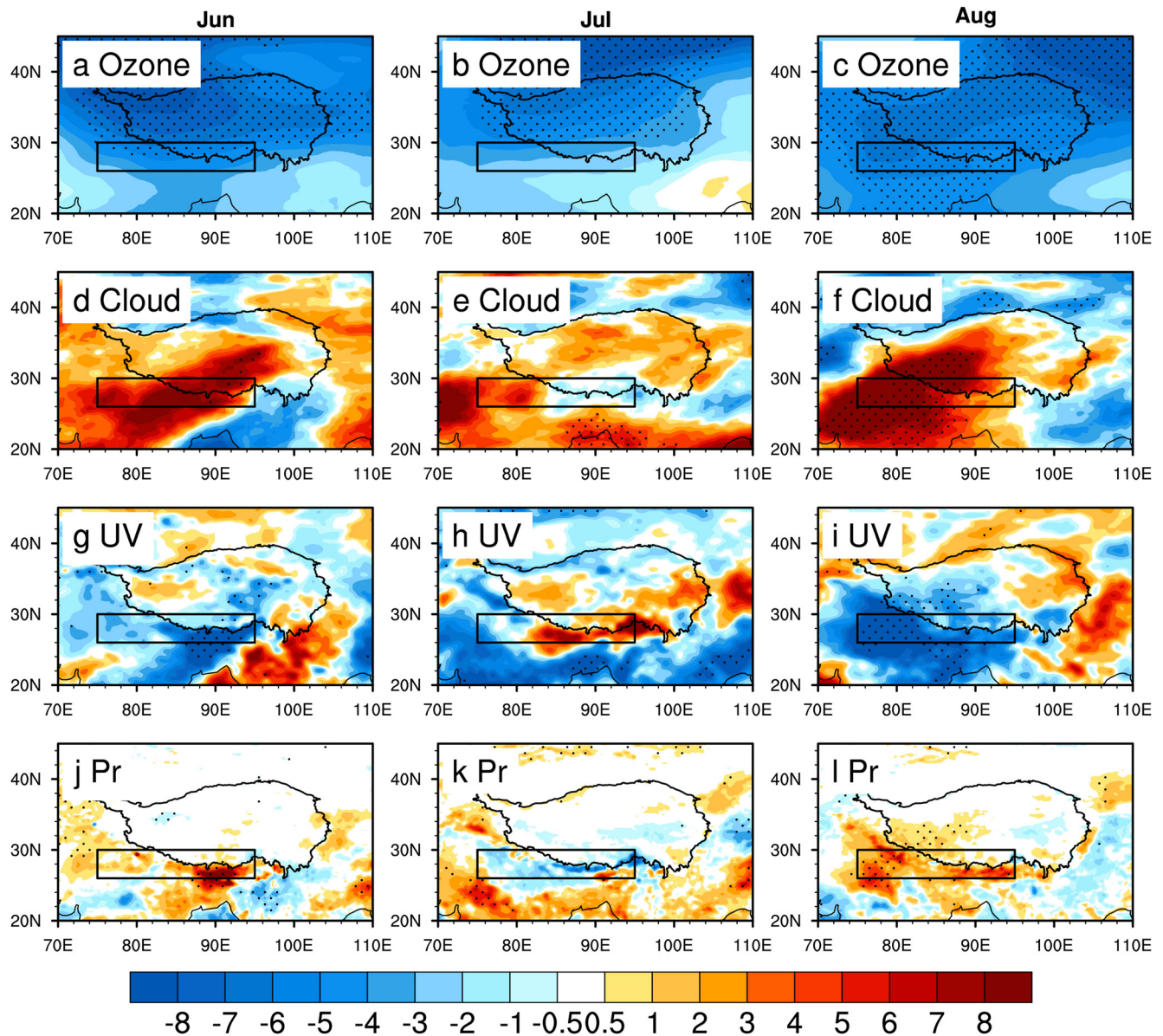


Figure 3. Geographic distributions of long-term trends of (a–c) total column ozone, (d–f) high clouds, (g–i) surface UV radiation, and (j–l) precipitation (Pr) during 1979–1996 in June (Jun), July (Jul), and August (Aug) based on ERA5 reanalysis. The unit of panels (a–c) is DU/decade, (d–f) is %/decade, (g–i) is $W\ m^{-2}/decade$, and then (j–l) is mm/day/decade, and they share the same colormap. Regions with dots are the places where regressions have statistical significance levels higher than the 95% confidence level based on the Student's t -test.

likely responsible for the increase in precipitation over the southern slope of the TP which can reach about 14.5, 7.9, and 12.9 mm/day/decade in June, July, and August, respectively (Figures 3j–3l). Note that the primary area of enhanced deep convection and increased precipitation in July is located further south than that in June and August.

Figures S5 and S6 in Supporting Information S1 further show the long-term trends during 1996–2022 in June, July, and August. We find that the ozone recovery during this period is located in the lower stratosphere between 70 and 15 hPa and accompanied by significant ozone depletion which centers at 100 hPa over 30°–40°N (Figures S5a–S5c in Supporting Information S1). The lower-stratospheric ozone depletion in recent two decades is consistent with the results in recent studies (Ball et al., 2018; Xie et al., 2023) which indicates that ozone has declined in the lower stratosphere since 1998 over 60°S–60°N. The trend of ozone recovery, which can reach about 0.5 ppm/decade, is smaller than the ozone depletion rate during 1979–1996 (−0.7 ppm/decade). The

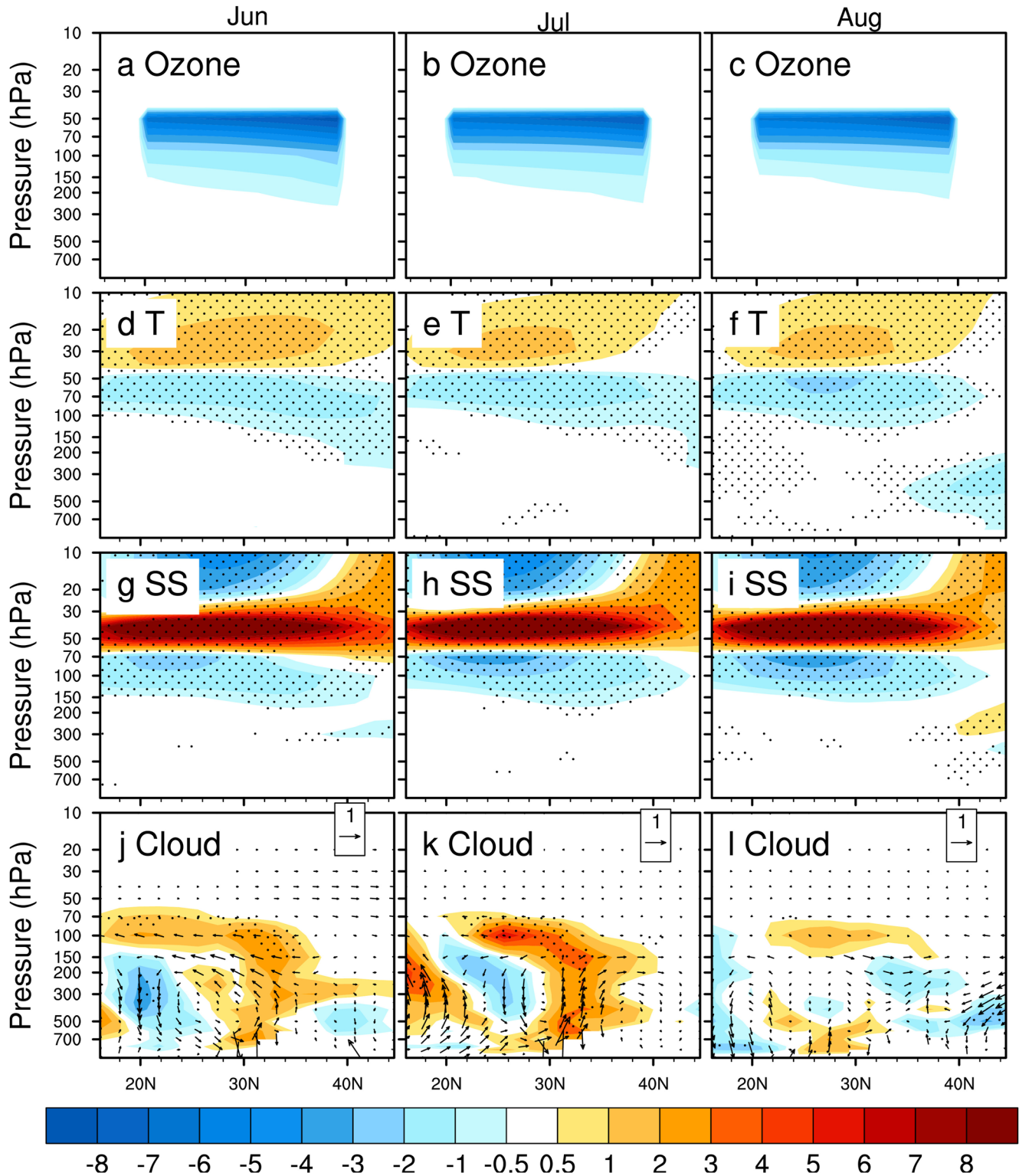


Figure 4. Climate responses to stratospheric ozone loss in model simulations. Vertical cross-section of (a–c) ozone changes and responses of (d–f) temperature (T), (g–i) static stability (SS), and (j–l) cloud cover (color contours) with winds (vectors) averaged over 75° – 95° E in June (Jun), July (Jul), and August (Aug) in CAM6 simulations. The unit of panels (a–c) is 10^{-1} ppm, (d–f) is K, (g–i) is 10^{-2} K/hPa, and then (j–l) is %, and they share the same colormap. In (j–l), the units are m/s and 10 hPa/day for the meridional and vertical winds, respectively. Regions with dots are the places where regressions have statistical significance levels higher than the 95% confidence level based on the Student's *t*-test.

radiative cooling effect of the lower-stratospheric ozone depletion at around 100 hPa weakens the stratospheric warming (Figures S5g–S5i in Supporting Information S1) caused by the above stratospheric recovery (Figures S5a–S5c in Supporting Information S1), which is consistent with the results (Figure 3) in Zhou et al. (2022). Thus, the associated stratospheric warming over 1996–2022 is much weaker than the magnitude of stratospheric cooling during 1979–1996 (Figures S5a–S5c in Supporting Information S1 vs. Figures 2a–2c). The significant warming is located at around 100 hPa south of 30°N with a maximum warming rate of 0.8 K/decade (Figures S5d–S5f in Supporting Information S1). It increases the static stability in the upper troposphere (Figures S5g–S5i in Supporting Information S1) and results in the weakening of deep convection and decrease in high clouds in the southern slope of the TP (Figures S5j–S5l and S6d–S6f in Supporting Information S1), which is consistent with the results during the period of stratospheric ozone depletion. The decrease in precipitation associated with the weakening of convection occurs in the southern slope of the TP in June and July and on the southeast side of the TP in July and August, with minimum values of -4.3 , -6.8 , and -6.2 mm/day/decade in June, July, and August, respectively (Figures S6j–S6l in Supporting Information S1). The decrease in high clouds leads to the increase of the surface UV radiation despite the ozone recovery, which has similar spatial pattern with the precipitation decrease (Figures S6d–S6l in Supporting Information S1). The sensitivity of the above results to the time periods chosen for ozone depletion and recovery has been tested (not shown here) and it is found that our results are not sensitive to the time periods chosen.

The ERA5 trend analyses indicate that the increase/decrease in stratospheric ozone over the TP is associated with the decrease/increase in convective precipitation over the southern slope of the TP. To further isolate the impact of the stratospheric ozone, we perform sensitivity experiments with different ozone prescriptions using a state-of-the-art atmospheric global climate model (GCM), CAM6. The simulations in the control experiment well reproduce the plenty amount of high clouds and heavy precipitation over the southern slope of the TP (Figures S7, S1, and S3 in Supporting Information S1).

Figure 4 shows the ozone changes and the responses of temperature, static stability, and clouds with winds averaged over 75°–95°E in June, July, and August from the simulations. The ozone loss, which peaks at about 50 hPa with a maximum reduction of about 0.8 ppm, leads to lower-stratospheric cooling between 100 and 50 hPa (Figures 4a–4f). This cooling has very similar spatial pattern and magnitude to that from the trend analyses (Figures 2a–2c), with a maximum cooling of about -2.1 K. The only difference is that significant warming occurs above the cooling between 40 and 10 hPa in the simulations due to the radiative warming induced by the more longwave absorption by the stratospheric ozone (Xia et al., 2018). We mainly focus on the lower-stratospheric temperature instead of the mid-stratospheric temperature which cannot affect the upper-tropospheric static stability. The lower-stratospheric cooling reduces the upper-tropospheric static stability (Figures 4g–4i) and results in the enhancement of the deep convection and consequent clouds increase at around 30°N (Figures 4g–4i).

Figure S8 in Supporting Information S1 shows the responses of high clouds, surface temperature, and precipitation to ozone loss in June, July, and August in CAM6. We find that the increase in high clouds associated with the ozone loss mainly occurs in the southwestern slope of the TP especially in June and July (Figures S8a–S8c in Supporting Information S1). The lower-stratospheric ozone depletion has little influence on surface temperature over the TP but leads to significant surface cooling in the southwestern slope of the TP (Figures S8d–S8f in Supporting Information S1). The enhancement of the deep convection results in significant increase of precipitation in the southwestern slope of the TP at around 30°N with maximum values of 2.5 and 3.3 mm/day in June and July, respectively (Figures S8g–S8i in Supporting Information S1), which is consistent with the results in the ERA5 (Figures 3j–3l). This precipitation change can reach about 14.3% of the multi-year average of the heavy precipitation in CAM6.

4. Conclusions and Discussions

Both the statistical and numerical analyses show that the decrease/increase of lower stratospheric ozone likely contributes to the increase/decrease in summer precipitation over the southern slope of the TP. We find this increase/decrease in precipitation is mainly caused by the enhancement/weakening of the deep convection associated with ozone depletion/recovery. For instance, stratospheric ozone loss cools the lower stratosphere and leads to a consequent decrease of static stability in the upper troposphere. This further results in enhancement of deep convection and more local high clouds over the southern slope of the TP where convective precipitation mostly occurs (Figure 5). We find that during the period of stratospheric ozone depletion (1979–1996),

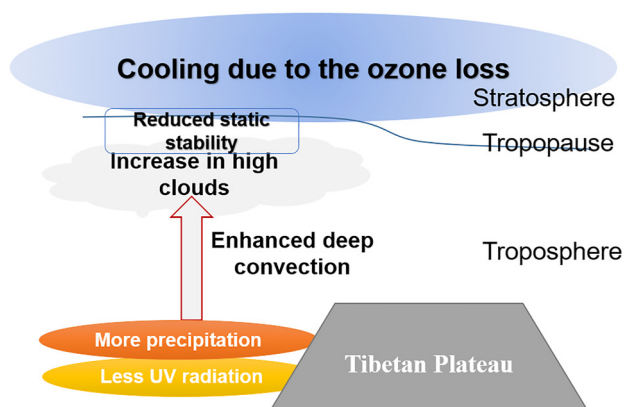


Figure 5. A schematic depiction of the climate impact of stratospheric ozone loss over the TP. The vertical and horizontal axes represent the altitude and the latitude, respectively.

precipitation over the southern slope of the TP had positive trends which can reach about 14.5, 7.9, and 12.9 mm/day/decade in June, July, and August in ERA5, respectively. In contrast, the negative trends of precipitation in ERA5, which can reach about -4.3 , -6.8 , and -6.2 mm/day/decade in June, July, and August, respectively, occurred during the period of stratospheric ozone recovery (1996–2022).

The above results are further verified by the sensitivity experiments using CAM6. It is found that the lower-stratospheric ozone depletion, which causes similar lower-stratospheric cooling to the long-term trends during 1979–1996 in the ERA5, results in the enhancement of deep convection and precipitation increase over the southwestern slope of the TP with maximum values of 2.5 and 3.3 mm/day in June and July, respectively in CAM6. The magnitudes of simulated precipitation changes are weaker than the trend analyses, which may be caused by the complex topographic conditions of the region, the coarse horizontal resolution, and biases from convective parameterization (Bao & Li, 2020).

As shown in Figures 2k and 3k, the primary area of enhanced deep convection and increased precipitation in July during 1979–1996 is located further south than that in June and August in the ERA5. In CAM6, the enhancement of the deep convection and increase of precipitation in response to stratospheric ozone depletion is much weaker in August than that in June and July (Figure 4l and Figure S8l in Supporting Information S1). These discrepancies among different months warrant further investigation in the future.

The cloud increase/decrease associated with the enhancement/weakening of convection causes the reduction/increase of the surface UV radiation in spite of the stratospheric ozone depletion/recovery, which is consistent with the recent study (Xia, Hu, Huang, Bian, & Zhao, 2021). The relationship between stratospheric ozone and high clouds and surface UV radiation is further examined using satellite observations. Figure S9 in Supporting Information S1 shows that high clouds are significantly negatively correlated with total column ozone in the southern slope of the TP, which is consistent with the results in the ERA5 reanalysis. The surface UV radiation is highly negatively correlated with total column ozone over the TP, which indicates that surface UV radiation is primarily controlled by the variation of stratospheric ozone in summer over the TP. The correlation coefficients between the surface UV radiation and total column ozone are significantly positive in the southern slope of the TP, which indicates that the indirect cloud effects may play an important role.

We find that the precipitation is significantly negatively correlated with the total column ozone in the southwestern slope of the TP especially in July and August in observations (Figures S9g–S9i in Supporting Information S1). This observed evidence further confirms that summer precipitation in the southern slope of the TP is closely related to stratospheric ozone variations, which has the potential to improve predictability of the precipitation. The lower stratospheric ozone reduction at around 100 hPa since 1996 (Figures S5a–S5c in Supporting Information S1) is likely to attenuate the decrease of the precipitation in the southern slope of the TP during 1996–2022 (Figures S6j–S6l in Supporting Information S1 vs. Figures 3j–3l). Further work is needed to examine how long this lower stratospheric ozone reduction will last.

Our results can help to improve the prediction of the precipitation over the southern slope of the Tibetan Plateau and ultimately reduce the uncertainty in our projections of future precipitation change. It suggests that more attention should be paid to the stratospheric ozone variations over the TP in summer especially future ozone recovery which may lead to less summer precipitation in the southern slope of the TP and is imperative for future water resource management for agriculture, hydroelectric generation, industrial development, and basic human needs in South Asia.

Data Availability Statement

The authors declare that datasets for this research are available in the following online repository. The ERA5 reanalysis available at <https://cds.climate.copernicus.eu/cdsapp#!/search?type=dataset&text=ERA5>. The MSR-2 reanalysis of the total column ozone can be found at www.temis.nl/protocols/O3global.html. The CERES

SYN1deg observations are available at <https://ceres-tool.larc.nasa.gov/ord-tool/jsp/SYN1degEd41Selection.jsp>. The OMI/Aura observations are obtained from <http://giovanni.gsfc.nasa.gov/giovanni/>. The GPCP monthly product is available at <https://psl.noaa.gov/data/gridded/data.gpcp.html>. The TRMM science data provided by NASA and Japan's National Space Development Agency are available at <https://gpm.nasa.gov/data/directory>. The CESM is available at <http://www.cesm.ucar.edu/models/cesm2/>. All computer codes generated during this study are available from the corresponding authors upon reasonable request.

Acknowledgments

We thank Dr Jian Yue for helpful comments. This work is supported by the Second Tibetan Plateau Scientific Expedition and Research Program (STEP), under grant of 2019QZKK0604, National Natural Science Foundation of China (42105016), and Key Laboratory of Middle Atmosphere and Global Environment Observation (LAGEO-2022-01). C. Zhao is supported by the National Natural Science Foundation of China, under Grants 41925022 and 91837204. Y. Hu is supported by the National Natural Science Foundation of China, under Grants 41888101, 41530423, and 41761144072. Y. Huang acknowledges a grant from the Natural Sciences and Engineering Research Council of Canada (RGPIN-2019-04511) and Canadian Space Agency (21SUASATHC).

References

- Adler, R. F., Huffman, G. J., Chang, A., Ferraro, R., Xie, P. P., Janowiak, J., et al. (2003). The version-2 global precipitation climatology project (GPCP) monthly precipitation analysis (1979–Present). *Journal of Hydrometeorology*, 4(6), 1147–1167. [https://doi.org/10.1175/1525-7541\(2003\)004<1147:tvGPCP>2.0.CO;2](https://doi.org/10.1175/1525-7541(2003)004<1147:tvGPCP>2.0.CO;2)
- Ball, W. T., Alsing, J., Mortlock, D. J., Staehelin, J., Haigh, J. D., Peter, T., et al. (2018). Evidence for a continuous decline in lower stratospheric ozone offsetting ozone layer recovery. *Atmospheric Chemistry and Physics*, 18(2), 1379–1394. <https://doi.org/10.5194/acp-18-1379-2018>
- Bandara, J. S., & Cai, Y. (2014). The impact of climate change on food crop productivity, food prices and food security in South Asia. *Economic Analysis and Policy*, 44(4), 451–465. <https://doi.org/10.1016/j.eap.2014.09.005>
- Bao, Q., & Li, J. (2020). Progress in climate modeling of precipitation over the Tibetan Plateau. *National Science Review*, 7(3), 486–487. <https://doi.org/10.1093/nsr/nwaa006>
- Cherchi, A., & Navarra, A. (2013). Influence of ENSO and of the Indian Ocean Dipole on the Indian summer monsoon variability. *Climate Dynamics*, 41(1), 81–103. <https://doi.org/10.1007/s00382-012-1602-y>
- Choudhury, G., Tyagi, B., Vissa, N. K., Singh, J., Sarangi, C., Tripathi, S. N., & Tesche, M. (2020). Aerosol-enhanced high precipitation events near the Himalayan foothills. *Atmospheric Chemistry and Physics*, 20(23), 15389–15399. <https://doi.org/10.5194/acp-20-15389-2020>
- Danabasoglu, G., Lamarque, J., Bacmeister, J., Bailey, D. A., DuVivier, A. K., Edwards, J., et al. (2020). The community earth system model version 2 (CESM2). *Journal of Advances in Modeling Earth Systems*, 12(2), e2019MS001916. <https://doi.org/10.1029/2019ms001916>
- Doelling, D. R., Loeb, N. G., Keyes, D. F., Nordeen, M. L., Morstad, D., Nguyen, C., et al. (2013). Geostationary enhanced temporal interpolation for CERES flux products. *Journal of Atmospheric and Oceanic Technology*, 30(6), 1072–1090. <https://doi.org/10.1175/jtech-d-12-00136.1>
- Doelling, D. R., Sun, M., Nguyen, L. T., Nordeen, M. L., Haney, C. O., Keyes, D. F., & Mlynczak, P. E. (2016). Advances in geostationary-derived longwave fluxes for the CERES synoptic (SYN1deg) product. *Journal of Atmospheric and Oceanic Technology*, 33(3), 503–521. <https://doi.org/10.1175/jtech-d-15-0147.1>
- Fasullo, J., & Webster, P. J. (2002). Hydrological signatures relating the Asian summer monsoon and ENSO. *Journal of Climate*, 15(21), 3082–3095. [https://doi.org/10.1175/1520-0442\(2002\)015<3082:hsrtas>2.0.CO;2](https://doi.org/10.1175/1520-0442(2002)015<3082:hsrtas>2.0.CO;2)
- Feng, L., & Zhou, T. (2012). Water vapor transport for summer precipitation over the Tibetan Plateau: Multidata set analysis. *Journal of Geophysical Research*, 117(D20), D20114. <https://doi.org/10.1029/2011jd017012>
- Gao, G., Chen, Q., Cai, H., Li, Y., & Wang, Z. (2019). Comprehensive characteristics of summer deep convection over Tibetan Plateau and its south slope from the global precipitation measurement core observatory. *Atmosphere*, 10(1), 9. <https://doi.org/10.3390/atmos10010009>
- Grossman, R. L., & Garcia, O. (1990). The distribution of deep convection over ocean and land during the Asian summer monsoon. *Journal of Climate*, 3(9), 1032–1044. [https://doi.org/10.1175/1520-0442\(1990\)003<1032:tdodco>2.0.CO;2](https://doi.org/10.1175/1520-0442(1990)003<1032:tdodco>2.0.CO;2)
- Hersbach, H., Bell, B., Berrisford, P., Hirahara, S., Horányi, A., Muñoz-Sabater, J., et al. (2020). The ERA5 global reanalysis. *The Quarterly Journal of the Royal Meteorological Society*, 146(730), 1999–2049. <https://doi.org/10.1002/qj.3803>
- Houze, R. A., Jr., Wilton, D. C., & Smull, B. F. (2007). Monsoon convection in the Himalayan region as seen by the TRMM precipitation radar. *The Quarterly Journal of the Royal Meteorological Society*, 133(627), 1389–1411. <https://doi.org/10.1002/qj.106>
- Hu, D., Guan, Z., & Tian, W. (2019). Signatures of the Arctic stratospheric ozone in northern Hadley circulation extent and subtropical precipitation. *Geophysical Research Letters*, 46(21), 12340–12349. <https://doi.org/10.1029/2019gl085292>
- Hu, Z., Lamraoui, F., & Kuang, Z. (2021). Influence of upper-troposphere stratification and cloud–radiation interaction on convective overshoots in the tropical tropopause layer. *Journal of the Atmospheric Sciences*, 78(8), 2493–2509. <https://doi.org/10.1175/jas-d-20-0241.1>
- Huangfu, J., Tang, Y., Ma, T., Chen, W., & Wang, L. (2021). Influence of the QBO on tropical convection and its impact on tropical cyclone activity over the western North Pacific. *Climate Dynamics*, 57(3), 657–669. <https://doi.org/10.1007/s00382-021-05731-x>
- Huffman, G. J., Adler, R. F., Bolvin, D. T., & Gu, G. (2009). Improving the global precipitation record: GPCP version 2.1. *Geophysical Research Letters*, 36(17), L17808. <https://doi.org/10.1029/2009gl040000>
- Huffman, G. J., Bolvin, D. T., Nelkin, E. J., Wolff, D. B., Adler, R. F., Gu, G., et al. (2007). The TRMM multisatellite precipitation analysis (TMPA): Quasi-Global, multiyear, combined-sensor precipitation estimates at fine scales. *Journal of Hydrometeorology*, 8(1), 38–55. <https://doi.org/10.1175/jhm560.1>
- Kim, H., Son, S.-W., & Yoo, C. (2020). QBO modulation of the MJO-related precipitation in East Asia. *Journal of Geophysical Research: Atmospheres*, 125(4), e2019JD031929. <https://doi.org/10.1029/2019jd031929>
- Lal, R. (2013). Food security in a changing climate. *Ecology and Hydrobiology*, 13(1), 8–21. <https://doi.org/10.1016/j.ecohyd.2013.03.006>
- Levelt, P. F., Oord, G. H. J. V. D., Dobber, M. R., Malkki, A., Huib, V., Johan de, V., et al. (2006). The ozone monitoring instrument. *IEEE Transactions on Geoscience and Remote Sensing*, 44(5), 1093–1101. <https://doi.org/10.1109/tgrs.2006.872333>
- Li, Y., Chipperfield, M. P., Feng, W., Dhomse, S. S., Pope, R. J., Li, F., & Guo, D. (2020). Analysis and attribution of total column ozone changes over the Tibetan Plateau during 1979–2017. *Atmospheric Chemistry and Physics*, 20(14), 8627–8639. <https://doi.org/10.5194/acp-20-8627-2020>
- Lim, Y., Son, S.-W., Marshall, A. G., Hendon, H. H., & Seo, K.-H. (2019). Influence of the QBO on MJO prediction skill in the subseasonal-to-seasonal prediction models. *Climate Dynamics*, 53(3), 1681–1695. <https://doi.org/10.1007/s00382-019-04719-y>
- Liu, H., Duan, K., Li, M., Shi, P., Yang, J., Zhang, X., & Sun, J. (2015). Impact of the North Atlantic Oscillation on the Dipole Oscillation of summer precipitation over the central and eastern Tibetan plateau. *International Journal of Climatology*, 35(15), 4539–4546. <https://doi.org/10.1002/joc.4304>
- Liu, X., & Yin, Z.-Y. (2001). Spatial and temporal variation of summer precipitation over the eastern Tibetan Plateau and the North Atlantic Oscillation. *Journal of Climate*, 14(13), 2896–2909. [https://doi.org/10.1175/1520-0442\(2001\)014<2896:satvos>2.0.CO;2](https://doi.org/10.1175/1520-0442(2001)014<2896:satvos>2.0.CO;2)
- Martin, Z., Son, S.-W., Butler, A., Hendon, H., Kim, H., Sobel, A., et al. (2021). The influence of the quasi-biennial oscillation on the Madden–Julian oscillation. *Nature Reviews Earth & Environment*, 2(7), 477–489. <https://doi.org/10.1038/s43017-021-00173-9>

- Nie, J., & Sobel, A. H. (2015). Responses of tropical deep convection to the QBO: Cloud-resolving simulations. *Journal of the Atmospheric Sciences*, 72(9), 3625–3638. <https://doi.org/10.1175/jas-d-15-0035.1>
- Qie, X., Wu, X., Yuan, T., Bian, J., & Lu, D. (2014). Comprehensive pattern of deep convective systems over the Tibetan Plateau–South Asian Monsoon region based on TRMM Data. *Journal of Climate*, 27(17), 6612–6626. <https://doi.org/10.1175/jcli-d-14-00076.1>
- Romatschke, U., & Houze, R. A. (2011). Characteristics of precipitating convective systems in the south Asian Monsoon. *Journal of Hydrometeorology*, 12(1), 3–26. <https://doi.org/10.1175/2010jhm1289.1>
- Romatschke, U., Medina, S., & Houze, R. A. (2010). Regional, seasonal, and diurnal variations of extreme convection in the south Asian Region. *Journal of Climate*, 23(2), 419–439. <https://doi.org/10.1175/2009jcli3140.1>
- Rutan, D. A., Kato, S., Doelling, D. R., Rose, F. G., Nguyen, L. T., Caldwell, T. E., & Loeb, N. G. (2015). CERES synoptic product: Methodology and validation of surface radiant flux. *Journal of Atmospheric and Oceanic Technology*, 32(6), 1121–1143. <https://doi.org/10.1175/jtech-d-14-00165.1>
- Schiemann, R., Lüthi, D., & Schär, C. (2009). Seasonality and interannual variability of the westerly jet in the Tibetan Plateau Region. *Journal of Climate*, 22(11), 2940–2957. <https://doi.org/10.1175/2008jcli2625.1>
- Seneviratne, S. I., Corti, T., Davin, E. L., Hirschi, M., Jaeger, E. B., Lehner, I., et al. (2010). Investigating soil moisture–climate interactions in a changing climate: A review. *Earth-Science Reviews*, 99(3), 125–161. <https://doi.org/10.1016/j.earscirev.2010.02.004>
- Sharma, S., Hamal, K., Khadka, N., & Joshi, B. B. (2020). Dominant pattern of year-to-year variability of summer precipitation in Nepal during 1987–2015. *Theoretical and Applied Climatology*, 142(3), 1071–1084. <https://doi.org/10.1007/s00704-020-03359-1>
- Son, S.-W., Lim, Y., Yoo, C., Hendon, H. H., & Kim, J. (2017). Stratospheric control of the Madden–Julian Oscillation. *Journal of Climate*, 30(6), 1909–1922. <https://doi.org/10.1175/jcli-d-16-0620.1>
- Turner, A. G., & Annamalai, H. (2012). Climate change and the South Asian summer monsoon. *Nature Climate Change*, 2(8), 587–595. <https://doi.org/10.1038/nclimate1495>
- Van Der A, R., Allaart, M., & Eskes, H. (2015a). Extended and refined multi sensor reanalysis of total ozone for the period 1970–2012. *Atmospheric Measurement Techniques*, 8(7), 3021–3035. <https://doi.org/10.5194/amt-8-3021-2015>
- Van Der A, R., Allaart, M., & Eskes, H. (2015b). *Multi-Sensor Reanalysis (MSR) of total ozone, version 2*. Royal Netherlands Meteorological Institute (KNMI).
- Wang, X., Pang, G., & Yang, M. (2018). Precipitation over the Tibetan plateau during recent decades: A review based on observations and simulations. *International Journal of Climatology*, 38(3), 1116–1131. <https://doi.org/10.1002/joc.5246>
- Webster, P. J., Magaña, V. O., Palmer, T. N., Shukla, J., Tomas, R. A., Yanai, M., & Yasunari, T. (1998). Monsoons: Processes, predictability, and the prospects for prediction. *Journal of Geophysical Research*, 103(C7), 14451–14510. <https://doi.org/10.1029/97jc02719>
- Xia, Y., Hu, Y., & Huang, Y. (2016). Strong modification of stratospheric ozone forcing by cloud and sea-ice adjustments. *Atmospheric Chemistry and Physics*, 16(12), 7559–7567. <https://doi.org/10.5194/acp-16-7559-2016>
- Xia, Y., Hu, Y., Huang, Y., Bian, J., & Zhao, C. (2021). Stratospheric ozone loss-induced cloud effects lead to less surface ultraviolet radiation over the Siberian Arctic in spring. *Environmental Research Letters*, 16(8), 084057. <https://doi.org/10.1088/1748-9326/ac18e9>
- Xia, Y., Hu, Y., Huang, Y., Zhao, C., Xie, F., & Yang, Y. (2021). Significant contribution of severe ozone loss to the Siberian–Arctic surface warming in spring 2020. *Geophysical Research Letters*, 48(8), e2021GL092509. <https://doi.org/10.1029/2021gl092509>
- Xia, Y., Hu, Y., Liu, J., Huang, Y., Xie, F., & Lin, J. (2020). Stratospheric ozone-induced cloud radiative effects on Antarctic sea ice. *Advances in Atmospheric Sciences*, 37(5), 505–514. <https://doi.org/10.1007/s00376-019-8251-6>
- Xia, Y., Huang, Y., & Hu, Y. (2018). On the climate impacts of upper tropospheric and lower stratospheric ozone. *Journal of Geophysical Research: Atmospheres*, 123(2), 730–739. <https://doi.org/10.1002/2017jd027398>
- Xie, F., Xia, Y., Feng, W., & Niu, Y. (2023). Increasing surface UV radiation in the tropics and northern mid-latitudes due to ozone depletion after 2010. *Advances in Atmospheric Sciences*, 1–11. <https://doi.org/10.1007/s00376-023-2354-9>
- Yao, B., Teng, S., Lai, R., Xu, X., Yin, Y., Shi, C., & Liu, C. (2020). Can atmospheric reanalyses (CRA and ERA5) represent cloud spatiotemporal characteristics? *Atmospheric Research*, 244, 105091. <https://doi.org/10.1016/j.atmosres.2020.105091>
- Yoo, C., & Son, S.-W. (2016). Modulation of the boreal wintertime Madden–Julian oscillation by the stratospheric quasi-biennial oscillation. *Geophysical Research Letters*, 43(3), 1392–1398. <https://doi.org/10.1002/2016gl067762>
- Yoshida, K., & Mizuta, R. (2021). Do sudden stratospheric warmings boost convective activity in the tropics? *Geophysical Research Letters*, 48(16), e2021GL093688. <https://doi.org/10.1029/2021gl093688>
- Zhang, C., & Zhang, B. (2018). QBO–MJO connection. *Journal of Geophysical Research: Atmospheres*, 123(6), 2957–2967. <https://doi.org/10.1002/2017jd028171>
- Zhang, G. J., & McFarlane, N. A. (1995). Sensitivity of climate simulations to the parameterization of cumulus convection in the Canadian climate centre general circulation model. *Atmosphere–Ocean*, 33(3), 407–446. <https://doi.org/10.1080/07055900.1995.9649539>
- Zhao, C., Yang, Y., Fan, H., Huang, J., Fu, Y., Zhang, X., et al. (2019). Aerosol characteristics and impacts on weather and climate over the Tibetan Plateau. *National Science Review*, 7(3), 492–495. <https://doi.org/10.1093/nsr/nwz184>
- Zhou, L., Xia, Y., & Zhao, C. (2022). Influence of Stratospheric ozone changes on stratospheric temperature trends in recent decades. *Remote Sensing*, 14(21), 5364. <https://doi.org/10.3390/rs14215364>
- Zou, M., Xiong, X., Wu, Z., & Yu, C. (2020). Ozone trends during 1979–2019 over Tibetan Plateau derived from satellite observations. *Frontiers in Earth Science*, 8. <https://doi.org/10.3389/feart.2020.579624>